



21st IAEA Fusion Energy Conference  
Chengdu, China, 16 - 21 October, 2006

---

IAEA-CN-149/ FT/P5-24

Minimization of the External Heating Power  
by Long Fusion Power Rise-up Time  
for Self-ignition Access  
in the Helical Reactor FFHR2m

O. Mitarai et al.

NIFS-867

Oct. 2006

## Minimization of the External Heating Power by Long Fusion Power Rise-up Time for Self-ignition Access in the Helical Reactor FFHR2m

O. Mitarai 1), A.Sagara 2), H.Chikaraishi 2), S.Imagawa 2), A.A.Shishkin 2)3) and O. Motojima 2)

- 1) Institute of Industrial Science and Technical Research, Kyushu Tokai University, 9-1-1 Toroku, Kumamoto 862-8652, Japan
- 2) National Institute for Fusion Science, 322-6 Oroshi-cho, Toki, 509-5292, Japan
- 3) Permanent address: Institute of Plasma Physics, National Science Center, ‘Kharkov Institute of Physics and Technology’, Kharkov-108, (310108), Ukraine

E-mail contact of main author: [omitarai@ktml.ktokai-u.ac.jp](mailto:omitarai@ktml.ktokai-u.ac.jp)

**Abstract** Minimization of the external heating power to access self-ignition is advantageous to increase the reactor design flexibility and to reduce the capital and operating costs of the plasma heating device in a helical reactor. In this work we have discovered that a larger density limit leads to a smaller value of the required confinement enhancement factor, lower density limit margin reduces the external heating power, and over 300 s of the fusion power rise-up time makes it possible to reach a minimized heating power. While the fusion power rise-up time in a tokamak is limited by the OH transformer flux or the current drive capability, any fusion power rise-up time can be employed in a helical reactor for reducing the thermal stresses of the blanket and shields, because the confinement field is generated by the external helical coils.

### 1. Introduction

While system codes analyzing the steady state plasma parameters have been used for stellarator reactors[1][2], we have been studying temporal evolutions of these parameters in helical reactors [3]-[6]. Recently based on the large helical device LHD ( $\bar{a}=0.6$  m,  $B_0=3$  T) experiments, we have determined the FFHR2m reactor size using the LHD size scaling including the blanket thickness and machine weight. FFHR2m reactor with the major radius  $R=14$  m and the coil pitch parameter  $\gamma=1.15$  provides the blanket thickness of 1.2 m for the given minor radius  $\bar{a}$ . In this machine ignition is possible for the confinement factor of 2.16 for the density limit factor of  $\gamma_{\text{SUDO}}=1.0$  over the Sudo density limit (proportional to the square root of the net heating power) [7]. If the density limit factor is improved to  $\gamma_{\text{SUDO}}=1.5$ , which is less than the observed value of 1.8 in LHD experiments, the confinement factor required for ignition can be reduced to 1.92 due to expansion of the operating density regime [6]. During the ignition access phase the external heating power is applied to increase the density limit, and the fusion power is linearly increased by controlling a fueling rate. The external heating power depends on the various parameters, such the confinement, impurity contents, the density limit factor and its operating margin, and fusion power rise-up time etc. In this paper, we demonstrate the effect of the density limit margin and the long fusion power rise-up time with more than 300 s on minimizing the external heating power to reach self-ignition using the zero-dimensional approach with the density and temperature profiling factors without the helical ripple effect [6], while other parameters are the same. We also show that any fusion power rise-up time is possible in a helical reactor if the large heating power is equipped.

## 2. Zero-dimensional equations with ignition control algorithm

In this analysis, the global power balance equation is used,

$$\frac{dW}{dt} = P_{EXT} - (P_L + P_B + P_S - P_\alpha) \quad (1)$$

where  $P_L$  is the total plasma conduction loss,  $P_B$  is the total bremsstrahlung loss,  $P_S$  is the total synchrotron radiation loss, and  $P_\alpha$  is the total alpha heating power. POPCON is the contour map of the heating power of  $P_{HT} = (P_L + P_B + P_S - P_\alpha)$  plotted on the n-T plane. The external heating power to expand the density limit, which is derived from the Sudo density limit, is given by

$$P_{EXT} [W] = \left\{ \gamma_{pr} \frac{(\gamma_{DLM} n(0) [m^{-3}])^2}{\gamma_{SUDO} 0.25 \times 10^{20}} \right\}^2 \frac{\bar{a}^2 R [m]}{B_o [T]} \times 10^6 - (P_\alpha - P_B - P_S) \quad (2)$$

where the set value of the minimum density limit margin (DLM) is  $\gamma_{DLMmin} = [n(0)_{limit}/n(0)]_{min} = 1.1$ , the profile factor is  $\gamma_{pr} = \bar{n}/n(0) = 2/3$  for the parabolic profile, and the density limit factor  $\gamma_{SUDO}$  over the Sudo density limit is  $\gamma_{SUDO} = 1.5$  in this study. Here,  $[n(0)_{limit}/n(0)]$  is called the density limit margin, which changes during the discharge. It is understood from Eq.(2) that when the density limit margin  $\gamma_{DLM}$  is large, the external heating power is increased. When the density limit factor  $\gamma_{SUDO}$  is large, the external heating power can be reduced.

In the D-T particle balance equation, the proportional-integration-derivative (PID) control of D-T fueling is used for feedback control of the fusion power. The helium ash confinement time ratio of  $\tau_\alpha^*/\tau_E = 3$  has been used in the helium ash particle balance equation. The ISS95 confinement scaling [8] is used for the plasma conduction loss.

$$\begin{cases} \tau_E [s] = \gamma_{ISS} \tau_{ISS95} [s] = \gamma_{LHD} \times 1.6 \tau_{ISS95} [s] \\ \tau_{ISS95} [s] = 0.079 \tau_{2/3}^{0.4} \bar{n}_{19}^{0.51} [\times 10^{19} m^{-3}] B_o^{0.83} [T] \bar{a}^{2.21} [m] R^{0.65} [m] / P_{HT}^{0.59} [MW] \end{cases} \quad (3)$$

where  $\gamma_{ISS}$  and  $\gamma_{LHD}$  represent the confinement enhancement factors over the ISS95 and present LHD scalings, respectively.

Engineering and physics designs of the helical reactor FFHR2m based on LHD have been progressing [6], whose birds-eye view is shown in Fig. 1. Machine and ignition plasma parameters on the steady state value are listed in Table 1.

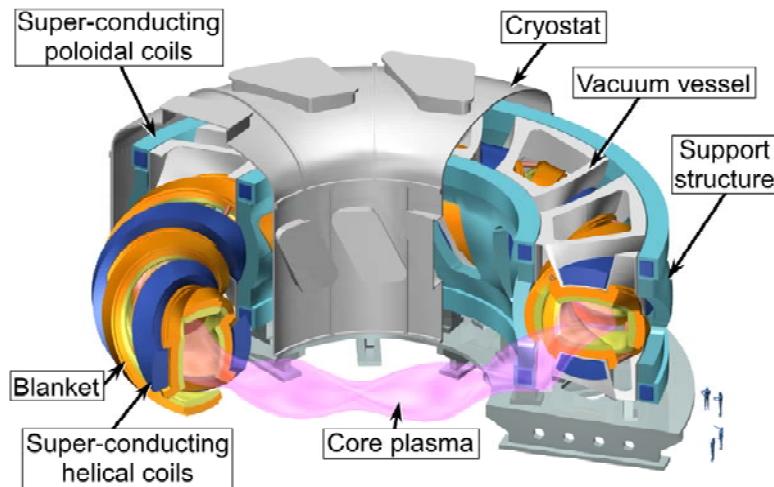


FIG.1 Birds-eye view of FFHR2m helical reactor

Table 1. Machine and ignition plasma parameters

		Steady state value
Major radius	R (m)	14.0
Effective minor radius	$\bar{a}$ (m)	1.73
Polarity/Field period	$\ell$ /m	2/10
Coil pitch parameter	$\gamma$	1.15
Magnetic field	$B_o$ (T)	6.0
Maximum magnetic field	$B_{o,max}$ (T)	13.3
Coil current density	$J_c$ (MA/m <sup>2</sup> )	26.6
Coil magnetic energy	$W_c$ (GJ)	120
Blanket thickness	$\Delta B$ (m)	1.2
Rotational transform	$t_{2/3}$	0.92
Maximum external heating power	$P_{EXT}$ (MW)	100
Confinement factor over ISS95 scaling	$\gamma_{ISS}$	1.92
Confinement time	$\tau_E$ (s)	1.9
Helium ash fraction	$F_{alpha}$	0.034
Oxygen impurity fraction	$F_o$	0.0075
Effective ion charge	$Z_{eff}$	1.48
He ash confinement time ratio	$\tau_{\alpha}^*/\tau_E$	3
Fusion alpha heating efficiency	$\eta_{\alpha}$	0.9
Operation density	$n_e(0)$ ( $10^{20}$ m <sup>-3</sup> )	2.8
Density limit factor over Sudo scaling	$\gamma_{SUDO}$	1.5
Density limit margin in the steady state	$[n(0)_{limit}/n(0)]$	1.27
Ion temperature	$T_i(0)$ (keV)	15.3
Ion to electron temperature ratio	$T_i/T_e$	1.0
Density profile	$\alpha_n$	1.0
Temperature profile	$\alpha_T$	1.0
Beta value	$\langle\beta\rangle$ (%)	3.0
Fusion power	$P_f$ (MW)	1900
Neutron power	$P_n$ (MW)	1520
Bremsstrahlung power	$P_B$ (MW)	57
Synchrotron radiation power	$P_S$ (MW)	3.4
Plasma conduction power	$P_L$ (MW)	282
Electric power output (thermal efficiency)	$P_e$ (MW)	627 (33%)
Neutron wall loading	$\Gamma_n$ (MW/m <sup>2</sup> )	1.5
Heat flux to first wall	$\Gamma_h$ (MW/m <sup>2</sup> )	0.06
Heat flux to divertor for 1m wet width	$\Gamma_{div}$ (MW/m <sup>2</sup> )	1.6
Energy multiplication ( $P_e/P_{EXT}$ )	$Q_E$	$\infty$

### 3. Ignition access and the heating power

Increase in the density limit factor can also reduce the confinement enhancement factor appreciably, because the density limit regime narrows the accessible ignition boundary in the lower density regime. The density limit factor of  $\gamma_{\text{SUDO}}=1.5$  employed in this analysis and the confinement factor of 1.92 are assumed to be constant during entire discharge.

Figure 2 shows the temporal evolution of plasma parameters of FFHR2m with  $R=14$  m,  $\bar{a}=1.73$  m,  $B_0=6$  T,  $P_f=1.9$  GW,  $\gamma_{\text{SUDO}}=1.5$ ,  $\gamma_{\text{ISS}}=1.92$  ( $\gamma_{\text{LHD}}=1.2$ ) and the helium ash confinement time ratio of  $\tau_{\alpha^*}/\tau_E=3$ . As the density limit margin is set to 1.1 at  $t=100$  s (DLM in Fig. 2-(c)) before the fusion power rise-up phase, the external heating power is increased from the preprogrammed value of 70 MW to 100 MW when the feedback control of the fusion power is switched on at 38 sec to adjust it to the preset fusion power. And then, the external heating power is automatically switched off at 100 s, showing self-ignition. The peak density at the steady state is  $2.67 \times 10^{20} \text{ m}^{-3}$ , the density limit is 27% over the operation density, the ion temperature is 15.8 keV, and the average neutron wall loading is  $1.5 \text{ MW/m}^2$ . Beta value is 3 % which is already achieved in LHD experiments.

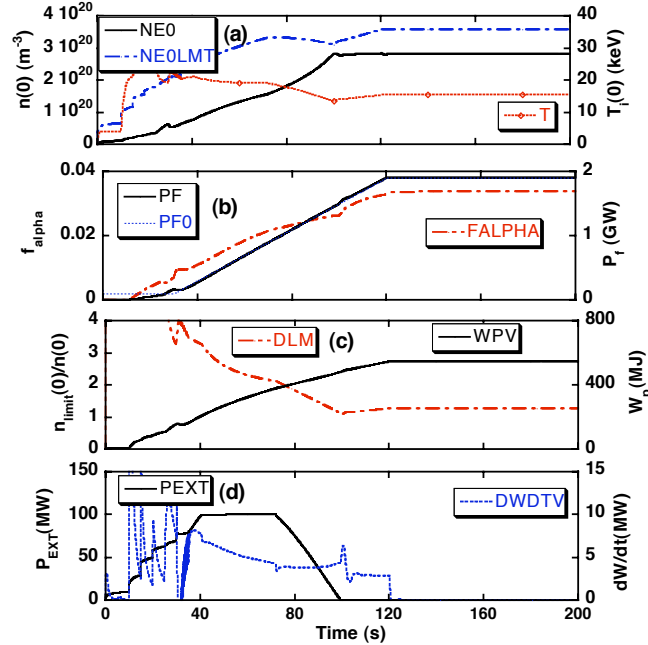


FIG. 2. Temporal evolution of plasma parameters in FFHR2m with the large pre-programming power of  $P_{\text{EXT-pre}}=70$  MW and  $\tau_{\text{rise}}=120$  sec. (a) The peak ion temperature  $T$ , the peak density  $NEO$ , the density limit  $NEOLMT$ , (b) the alpha ash fraction  $FALPHA$ , the fusion power  $PF$ , its set value  $PF0$ , (c) the density limit margin  $DLM$  ( $=NEOLMT/NEO$ ), the plasma energy  $WPV$ , and (d) the external heating power  $PEXT$  and the time derivative of the plasma energy  $DW/dt$ .

In Fig. 2, the operating density is much lower than the density limit (Fig.2-(a)) with  $\gamma_{\text{SUDO}}=1.5$ , then the density limit margin  $DLM$  ( $=NEOLMT/NEO$ ) is much larger than 1.0 during the fusion power rise-up phase. Therefore, when the initial pre-programming power is reduced to 40 MW as shown in Fig. 3, the density limit margin is reduced to less than 2 during the fusion power rise-up phase, and then the feedback controlled external heating power is also reduced to 50 MW even for the shorter fusion power rise-up time of 120 sec. The time derivative of the plasma energy is  $dW/dt=5\sim 10$  MW during the fusion power rise-up phase.

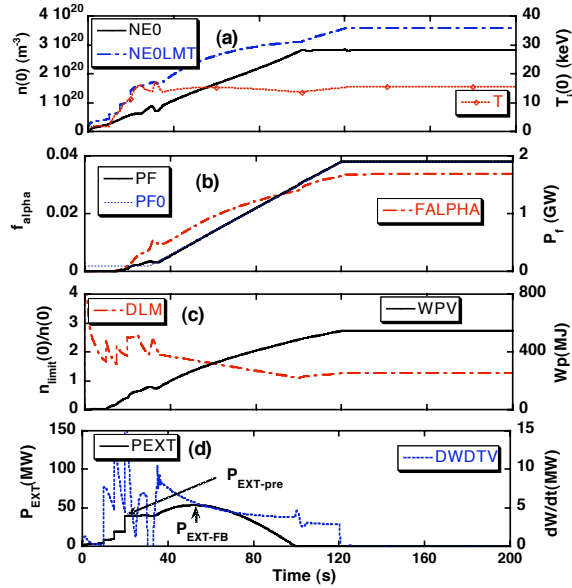


FIG. 3. Temporal evolution of plasma parameters with the smaller pre-programming power of  $P_{EXT-pre}=40$  MW and  $\tau_{rise}=120$  sec.

In the following the density limit margin is set to 1.1 at  $t=100$  s as above. When the fusion power rise-up time is further extended to 300 sec as shown in Fig. 4, where the initial pre-programming power is further reduced to 25 MW, the external heating power is further reduced to 32 MW. In this case, the density limit margin still plays a role to determine the external heating power, because the maximum heating power takes place within 100 s.  $dW/dt$  is 3~10 MW during the fusion power rise-up phase.

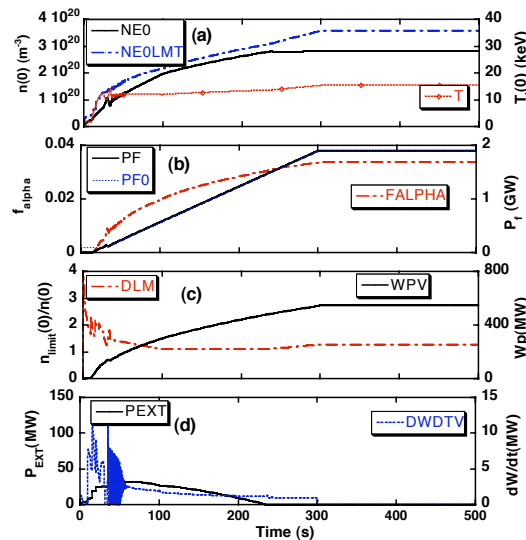


FIG. 4. Temporal evolution of plasma parameters with the pre-programming power of  $P_{EXT-pre}=25$  MW and  $\tau_{rise}=300$  sec.

When the fusion power rise-up time is further extended to 7200 s (two hours), the external heating power can be reduced to 27 MW for the initial pre-programming power of 25 MW as shown in Fig. 5. The density limit margin does not determine the heating power any more in this case so that the heating power reaches the maximum at 1000 s. The  $dW/dt$  value is almost negligible during the fusion power rise-up phase.

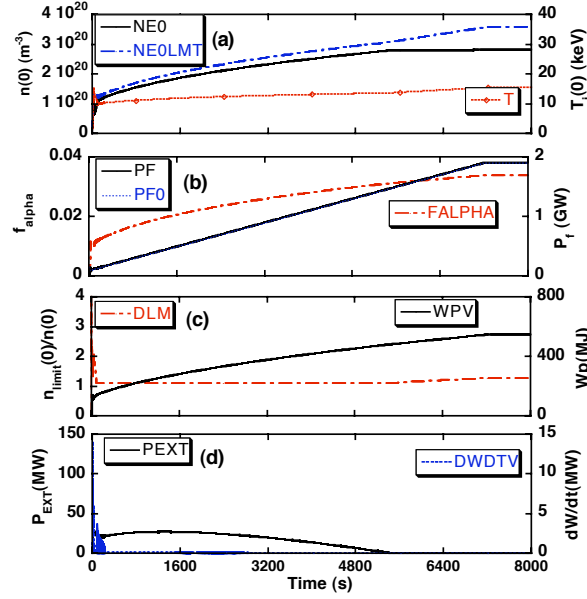


FIG.5. Temporal evolution of plasma parameters with the pre-programming power of  $P_{\text{EXT-pre}}=25$  MW a long fusion power rise-up time of  $\tau_{\text{rise}}=7200$  sec.

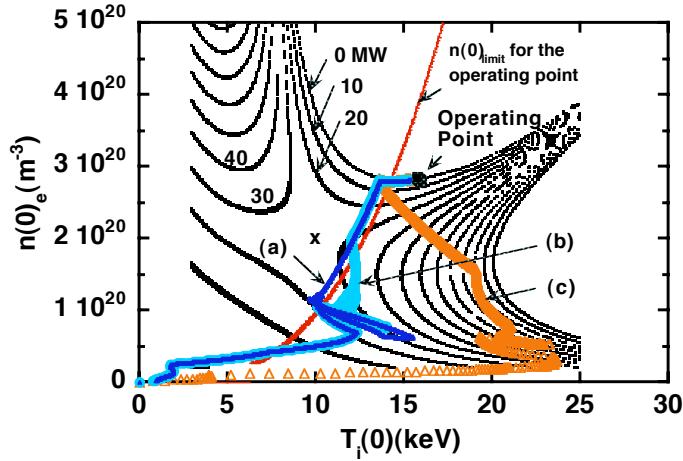


FIG.6. Three operation paths to ignition point on POPCON diagram for (a)  $\tau_{\text{rise}}=2$  hours and  $P_{\text{EXT-pre}}=25$  MW (corresponding to Fig. 5), (b)  $\tau_{\text{rise}}=300$  sec and  $P_{\text{EXT-pre}}=25$  MW (Fig. 4), and (c)  $\tau_{\text{rise}}=120$  sec and  $P_{\text{EXT-pre}}=70$  MW (Fig.2). The exact density limit ( $n(0)_{\text{limit}}$ ) for the final operating point at  $P_{\text{EXT}}=0$  MW is pointed by arrow. Above the density limit line, there is no accessible regime. "X" indicates the saddle point.

In Fig. 6 are shown three operation paths to ignition point on POPCON diagram for (a)  $\tau_{\text{rise}}=2$  hours and  $P_{\text{EXT-pre}}=25$  MW (corresponding to Fig. 5), (b)  $\tau_{\text{rise}}=300$  sec and  $P_{\text{EXT-pre}}=25$  MW (Fig. 4), and (c)  $\tau_{\text{rise}}=120$  sec and  $P_{\text{EXT-pre}}=70$  MW (Fig.2). The operating path goes near the saddle point in the case (a) with the long fusion power rise-up time. Operation path with the shorter fusion power rise-up time (case (b)) makes a small detour around the saddle point mainly due to the larger heating power determined by the density limit margin. In the shortest rise-up time (case (c)) the operating point climbs up to the higher heating power level on POPCON due to the larger density limit margin determined by the initial large preprogrammed heating power of 70 MW. We note that the contour lines and the

density limit line on POPCON is drawn for the final ignited operating point with  $P_{EXT}=0$  MW. This means that the density limit line is slightly shifted to higher density for the finite external heating power during the heating phase. In general when the operating point passes on the saddle point on POPCON, the heating power is minimum. However, as seen in Fig. 6, as an inaccessible density limit regime exists around the saddle point, the density limit margin plays an important role to reduce the heating power. Furthermore, as the long fusion power rise-up time provides the small  $dW/dt$  term in the power balance equation, the external heating power  $P_{EXT}$  can be reduced as understood from the rearranged power balance equation:

$$P_{EXT} = \frac{dW}{dt} + (P_L + P_B + P_S - P_\alpha) \quad (4)$$

In Fig. 7 feedback controlled heating powers (solid symbols) for various pre-programmed heating power (open symbols) are plotted for various fusion power rise-up times. Feedback controlled heating powers, which is influenced by the pre-programming heating power through the density limit margin, is larger than the pre-programmed heating power. Such situation was seen in Fig.3-(d). Thus, the effect of the density limit margin on the reduction of the external heating power is dominant in the shorter rise-up time range. When the fusion power rise-up time is longer than  $\sim 300$  sec or more and the pre-programming heating power is reduced to 25 MW, the density limit margin effect disappears and the heating power is further reduced to the minimum heating power of 27 MW.

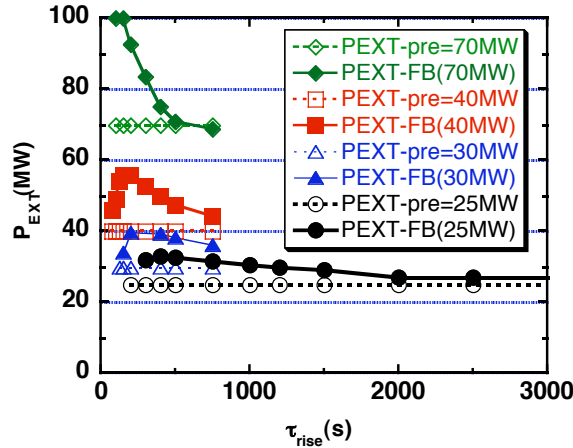


FIG. 7. The maximum feedback controlled heating powers (solid symbols,  $P_{EXT-FB}$ ) to reach self-ignition for various initial pre-programming powers (open symbols,  $P_{EXT-pre}=70, 40, 30,$  and 25 MW) in the case of various fusion power rise-up times.

#### 4. Discussions and summary

As shown in Fig. 7 even low pre-programming heating power allows reaching ignition with the lower density limit margin and the short fusion power rise-up time, where the time constant density limit factor  $\gamma_{SUDO}=1.5$  has been used. However, in a short fusion power rise-up time, the first wall and surface condition may not reach the steady state condition. As the plasma edge condition governing the density limit may not be established firmly in a short time, the density limit factor  $\gamma_{SUDO}$  could be varied and the actual density limit itself is unclear. Impurity, density and temperature profiles also may change during a short time fusion power rise-up phase. Therefore, setting of the larger safety margin for the density limit is better to ensure a discharge evolution with a short



fusion power rise-up time. On the other hand, in a long fusion power rise-up time, as the plasma wall interaction may be controlled under quasi-steady state conditions, the smaller density limit margin could be employed to reduce the external heating power.

In this study, we have discovered the fundamental fact on ignition access. The larger heating power is required to make a shorter fusion power rise-up time due to the  $dW/dt$  effect, yielding the longer operation path on POPCON. On the other hand, the smaller heating power needs the longer fusion power rise-up time to access ignition, leading to the shorter path to the operating point on POPCON. Thus, the shortest rise-up time does not correspond to the shortest path on POPCON during an ignition access.

We have studied how to reduce the external heating power in a helical reactor. From a new point of view, however, this reduction means that when the larger external heating power such as 100 MW or more is prepared, any fusion power rise-up time from short to long rise-up time can be available. It may provide the flexibility of the machine operation in a helical reactor, because of the short rise-up time for checking the plasma operation without waiting for the long time, and the long rise-up time to reduce the thermal stress in a blanket etc. This type of the flexibility may not be expected in a tokamak reactor because such a shorter fusion power rise-up time is limited in a transformer operation, and the non-inductive current drive operation is possible only at a very long fusion power rise-up time [9].

In this paper we demonstrated the effect of the density limit margin and the long fusion power rise-up time with more than 300 s on minimizing the external heating power to reach self-ignition. We also showed that any fusion power rise-up time is possible in a helical reactor if the large heating power is equipped.

This work is performed with the support and under the auspices of the NIFS Collaborative Research Program NIFS04KFDF001 and NIFS05ULAA116.

## References

- [1] BEIDLER, C. D., et al., "The Helias Reactor HRS4/18", IPP-report IPP-III/268, February 2001.
- [2] NAJIMABADI, F., "Overview of ARIES Compact Stellarator Study", US/Japan Workshop on Fusion Power Plant Studies and Advanced Technology with EU Participation, 24-25 January, 2006, San Diego USA.
- [3] MITARAI, O., SAGARA, A., SUDO, S., and MOTOJIMA, O., "Ignition Analysis on a High Field D-T Helical Reactor", *Fusion Technology* 27 (1995.5) 278-281
- [4] MITARAI, O., SAGARA, A., and MOTOJIMA, O., "Ignition Access in the FFHR D-T Helical Reactor", *J. of Plasma Fusion Res. SERIES*, 1 (1998) 418
- [5] MITARAI, O., ODA, A., SAGARA, A., YAMAZAKI, K., and MOTOJIMA, O., "Pellet Injection Algorithm for the FFHR Helical Reactor", *Fusion Engineering and Design* 70 (2004) 247
- [6] SAGARA A., IMAGAWA, S., MITARAI, O., DOLAN, T., TANAKA, T., KUBOTA, Y. et al., *Nucl. Fusion* 45 (2005) 258
- [7] SUDO, S., TAKEIRI, Y., ZUSHI, H., SANO, F., ITOH, K., KONDO, K., and IYOSHI, A., "Scalings of Energy Confinement and Density Limit in Stellarator/Heliotron Devices", *Nucl. Fusion* 30 (1990) 11
- [8] STROH, U., MURAKAMI, M., DORY, R. A., YAMADA, H., OKAMURA, S., SANO, F., and OBIKI, T., "Energy Confinement Scaling from International Stellarator Database", *Nucl. Fusion* 36, (1996) 1063
- [9] MITARAI, O., YOSHINO, R., and USHIGUSA, K., "Plasma current ramp-up assisted by outer vertical field coils in a high aspect ratio tokamak", *Nucl. Fusion* 10 (2002) 1257